Journal of Organometallic Chemistry, 303 (1986) 99–109
Elsevier Sequoia S.A., Lausanne – Printed in The Netherlands

X-RAY STRUCTURAL CHARACTERIZATION OF $[Et_4N^+]_3[BiFe_4(CO)_{16}^{3-}]$

MELVYN ROWEN CHURCHILL *, JAMES C. FETTINGER,
Department of Chemistry, University at Buffalo, State University of New York, Buffalo, NY 14214 (U.S.A.)

KENTON H. WHITMIRE and CRAIG B. LAGRONE
Department of Chemistry, Rice University, Houston, Texas 77251 (U.S.A)

(Received September 18th, 1985)

Summary

Sodium bismuthate has previously been reported to react with $Fe(CO)_5$ in methanolic KOH, producing the $[BiFe_4(CO)_{16}^{3-}]$ anion. $[Et_4N^+]_3[BiFe_4(CO)_{16}^{3-}]$ crystallizes in the centrosymmetric monoclinic space group $P2_1/n$ with a 13.497(2), b 19.765(3), c 19.275(3) Å, β 91.086(13)°, V 5141.0(15) Å^3, $Z = 4$. Diffraction data ($2\theta = 4.5$–$45.0°$, using Mo-K_α radiation) were collected with a Syntex $P2_1$ automated four-circle diffractometer and the structure was refined to R_F 7.5% and R_{wF} 6.1% for those 4306 reflections with $|F_o| > 3\sigma(|F_o|)$. The $[BiFe_4(CO)_{16}^{3-}]$ anion contains a central bismuth tetrahedrally surrounded by $Fe(CO)_4$ units, with an average Bi–Fe distance of 2.750(2) Å. Each iron atom is in a trigonal-bipyramidal environment. The three Et_4N^+ cations are all disordered.

Introduction

We have recently become interested in heteronuclear bismuth–iron cluster complexes and have reported the results of structural studies on the $[BiFe_3(CO)_9(\mu_3\text{-}CO)^-]$ anion [1], $Bi_2Fe_3(CO)_9$ [2] and the $[Bi_4Fe_4(CO)_{13}^{2-}]$ anion [3]. We also reported the synthesis of salts of the $[BiFe_4(CO)_{16}^{3-}]$ anion, but found that crystals of $[Me_4N^+]_3[BiFe_4(CO)_{16}^{3-}]$ were unsuitable for X-ray analysis [1]. This trianion is of interest for a number of reasons.

(1) It is one of a small number of homoleptic (carbonylmetalate) complexes of bismuth. Other well characterized examples are $Bi[Co(CO)_4]_3$ [4] and $Bi_2[W(CO)_5]_3$ [5], along with the related cluster complex $BiIr_3(CO)_9$ [6].

(2) It is one of a limited number of highly charged metal carbonyl cluster anions. Shore and coworkers have reported such highly charged tetranuclear ruthenium

* Address correspondence to this author.

0022-328X/86/$03.50

carbonyl cluster anions as $[Ru_4(CO)_{11}^{6-}]$ and $[Ru_4(CO)_{12}^{4-}]$ [7] but there are few other such examples.

We have now obtained crystals of $[Et_4N^+]_3[BiFe_4(CO)_{16}^{3-}]$ that are suitable for an X-ray diffraction study and which enable us to confirm the approximate T_d symmetry of the $[BiFe_4(CO)_{16}^{3-}]$ anion which was predicted from spectroscopic studies [1].

Experimental

The synthesis of $[Et_4N^+]_3[BiFe_4(CO)_{16}^{3-}]$ has previously been reported [1]. We wish to emphasize the following points concerning the synthesis of this compound. The synthesis is a clean, high yield procedure as long as air is rigorously excluded. The reaction is best carried out entirely in methanol. Although the complex is not moisture sensitive, it is more easily oxidized in the presence of water. The complex in solution is very air-sensitive prior to its isolation as the Et_4N^+ salt. The isolated solid, however, appears reasonably insensitive to air although it will decompose upon prolonged exposure.

The tetraalkylammonium salts are completely insoluble in methanol while the impurities dissolve readily, thereby affording a convenient method of purification. The product will react further with $NaBiO_3$, so excess should be avoided. Since commercial $NaBiO_3$ is technical grade (85%), care should be taken in making the final additions. This reaction of $[BiFe_4(CO)_{16}^{3-}]$ with $NaBiO_3$ produces oxidized, brown bismuth-containing metal carbonyls which are under investigation. The synthesis can be scaled up easily using the procedure previously described; with quantities of 1.0 g $NaBiO_3$ (85%), 2.0 ml $Fe(CO)_5$, and 2.0 g KOH, 3.9 g of $[Et_4N^+]_3[BiFe_4(CO)_{16}^{3-}]$ was obtained (83% based on iron).

The crystals used for the X-ray diffraction study were grown fortuitously from an acetone solution of the brown complex that results when excess $NaBiO_3$ is used in the preparation of the title complex. The crystals were shown by solubility studies, color and infrared spectroscopy to be the authentic green complex.

Collection of X-ray diffraction data for $[Et_4N^+]_3[BiFe_4(CO)_{16}^{3-}]$

The crystals selected for the crystallographic analysis was dark green in color with approximate orthogonal dimensions of $0.23 \times 0.27 \times 0.30$ mm^3. It was sealed into a thin walled glass capillary in air (following observations that the crystals appear to be stable for periods of > 3 d in air). The capillary was mounted on a eucentric goniometer and accurately centered on the Syntex $P2_1$ automated four-circle diffractometer at SUNY-Buffalo. All subsequent set-up operations (i.e., determination of the crystal's orientation matrix and unit cell dimensions) and data collection were performed as described previously [8]. Details are listed in Table 1.

A careful examination of the full data set revealed the systematic absences of $h0l$ for $h + l = 2n + 1$ and $0k0$ for $k = 2n + 1$; this is indicative of the centrosymmetric monoclinic space group $P2_1/n$. Data were corrected for the effects of absorption and for Lorentz and polarization factors. Symmetry-equivalent data were averaged and the data placed on an approximately absolute scale by means of a Wilson plot. Any datum with $I(\text{net}) < 0$ was expunged from the data file.

TABLE 1

EXPERIMENTAL DATA FOR THE X-RAY DIFFRACTION STUDY OF $[Et_4N^+]_3[BiFe_4(CO)_{16}^{3-}]$

(A) Unit cell data at 24°C (297 K)

Crystal system: monoclinic	V 5141.0(15) Å^3
Space group: $P2_1/n$ (No. 14)	Formula $C_{40}H_{60}O_{16}N_3BiFe_4$
a 13.497(2) Å	Mol. wt. 1271.4
b 19.765(3) Å	$Z = 4$
c 19.275(3) Å	D(calc'd) 1.64 g cm^{-3}
β 91.086(13)°	

(B) Measurement of intensity data

Diffractometer: Syntex $P2_1$

Radiation: Mo-K_α ($\bar{\lambda}$ 0.710730 Å)

Monochromator: pyrolitic graphite in equatorial mode with $2\theta_{max}$ 12.160° for 002 reflection; assumed to be 50% perfect/50% ideally mosaic for polarization correction

Reflections measured: $+h$, $+k$, $\pm l$ for $2\theta = 4.5$–$45.0°$, yielding 5696 unique data with $I > 0$. (File BIF2-210.)

Scan method: coupled θ(crystal)–2θ(counter) at a speed of 4.0 deg/min in 2θ, over the range $[2\theta(K_{\alpha_1}) - 1.0]°$ through $[2\theta(K_{\alpha_2}) + 1.0]°$

Background measurement: stationary-crystal and stationary counter at each end of the 2θ scan, each for 25% of scan time

Standard reflections: 3 approximately mutually orthogonal reflections were recollected after each 97 data points. A monotonic decrease to about 90% initial intensity was observed and corrected for.

Absorption: μ 44.4 cm^{-1}; data were corrected empirically by interpolation (in 2θ and ϕ) between transmission curves based upon ψ-scans of five close-to-axial reflections.

Solution and refinement of the crystal structure of $[Et_4N^+]_3[BiFe_4(CO)_{16}^{3-}]$

All calculations were performed on our in-house computer using our locally-modified version of the Syntex XTL interactive crystallographic program package [9]. The structure was solved by direct methods using the program MULTAN [5]; the 'E-map' of the phase-set of highest figure-of-merit revealed the five heavy atoms (i.e., the $BiFe_4$ core). The remaining atoms of the $[BiFe_4(CO)_{16}^{3-}]$ anion were easily located from difference-Fourier maps. Atoms of the three $[Et_4N^+]$ cations were located with rather more difficulty. At first it seemed that these were ordered, but thermal parameters of the α-carbon atoms (B 16–22 Å^2) were uniformly much higher than those of the β-carbon atoms (B 6–11 Å^2). This immediately suggested disorder of the $[Et_4N^+]$ cations as shown in Scheme 1. A difference-Fourier map revealed very weak features corresponding to the probable secondary locations of the disordered α-carbon atoms. Continued refinement showed that, for each cation,

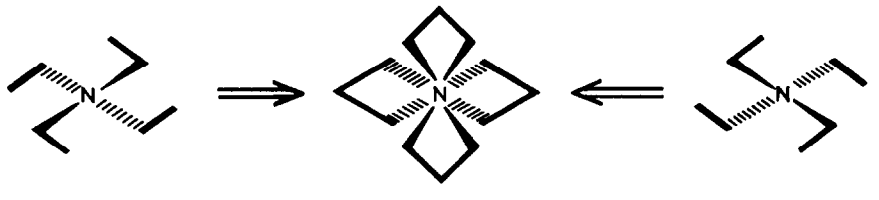

SCHEME 1

TABLE 2

FINAL POSITIONAL PARAMETERS FOR $[Et_4N^+]_3[BiFe_4(CO)_{16}^{3-}]$

Atom	x	y	z	B (Å^2)
(A) Atoms of the $[BiFe_4(CO)_{16}^{3-}]$ anion				
Bi	−0.01464(4)	0.24895(5)	0.22798(3)	
Fe(1)	−0.20532(18)	0.28851(14)	0.19499(13)	
Fe(2)	0.10153(16)	0.25129(19)	0.11243(11)	
Fe(3)	0.06341(18)	0.33645(13)	0.32564(13)	
Fe(4)	−0.01433(18)	0.12082(13)	0.28343(13)	
O(11)	−0.1383(11)	0.42859(78)	0.20603(92)	
O(12)	−0.2704(11)	0.20855(80)	0.31454(87)	
O(13)	−0.1921(10)	0.21879(88)	0.06120(79)	
O(14)	−0.4064(11)	0.33487(82)	0.17477(77)	
O(21)	0.0472(12)	0.10975(82)	0.08819(73)	
O(22)	−0.0128(11)	0.36784(88)	0.06386(80)	
O(23)	0.2762(10)	0.27010(77)	0.20261(76)	
O(24)	0.2146(10)	0.2528(11)	−0.01525(69)	
O(31)	0.1044(12)	0.43134(79)	0.21204(81)	
O(32)	0.2079(10)	0.23080(68)	0.36429(75)	
O(33)	−0.13327(94)	0.33894(80)	0.39194(78)	
O(34)	0.1386(11)	0.42310(80)	0.43491(81)	
O(41)	−0.0664(11)	0.18048(70)	0.41565(77)	
O(42)	−0.1620(12)	0.08704(83)	0.17639(92)	
O(43)	0.1962(10)	0.10846(77)	0.25046(90)	
O(44)	−0.0307(14)	−0.00985(81)	0.34643(88)	
C(11)	−0.1594(15)	0.3713(11)	0.2028(10)	4.65(46)
C(12)	−0.2428(13)	0.2386(11)	0.26890(91)	4.24(42)
C(13)	−0.1925(13)	0.2455(13)	0.1133(10)	5.15(42)
C(14)	−0.3244(16)	0.3163(11)	0.1802(10)	4.92(46)
C(21)	0.0646(15)	0.1652(12)	0.0999(11)	4.70(49)
C(22)	0.0299(15)	0.3215(11)	0.0871(10)	4.02(44)
C(23)	0.2050(13)	0.26560(93)	0.16809(90)	4.01(42)
C(24)	0.1697(13)	0.2533(14)	0.03554(93)	4.88(40)
C(31)	0.0895(15)	0.3903(11)	0.2548(11)	4.75(51)
C(32)	0.1483(14)	0.2711(10)	0.3466(10)	4.10(45)
C(33)	−0.0624(16)	0.3344(11)	0.3631(11)	4.72(51)
C(34)	0.1096(14)	0.3866(10)	0.3878(10)	4.21(42)
C(41)	−0.0453(16)	0.1588(11)	0.3609(11)	4.60(50)
C(42)	−0.1023(14)	0.1019(10)	0.2188(10)	4.14(44)
C(43)	0.1144(16)	0.1161(11)	0.2637(11)	4.45(48)
C(44)	−0.0206(16)	0.0425(12)	0.3196(11)	5.43(50)
(B) Atoms of the $[Et_4N^+]$ cations				
N(1)	0.2569(11)	0.50389(75)	0.01746(80)	4.19(32)
N(2)	1.0053(12)	0.61304(86)	0.37752(85)	4.88(37)
N(3)	0.4596(11)	0.38032(81)	0.37387(79)	4.36(34)
C(1A)	0.2338(29)	0.5229(21)	0.0975(20)	7.5(10)
C(1AA)	0.1496(45)	0.5319(33)	0.0122(31)	9.4(16)
C(2A)	0.1622(29)	0.4615(21)	−0.0068(21)	8.5(10)
C(2AA)	0.2772(43)	0.4788(32)	−0.0574(31)	6.5(15)
C(3A)	0.3509(29)	0.4604(21)	0.0236(20)	6.6(10)
C(3AA)	0.2471(44)	0.4371(31)	0.0793(31)	8.1(15)
C(4A)	0.2709(28)	0.5664(21)	−0.0322(21)	5.4(10)

TABLE 2 (continued)

Atom	x	y	z	B (Å^2)
C(4AA)	0.3423(46)	0.5509(32)	0.0472(33)	6.3(16)
C(5A)	0.1408(23)	0.5747(16)	0.0902(17)	11.30(91)
C(6A)	0.1966(20)	0.4301(14)	−0.0847(15)	9.21(77)
C(7A)	0.3432(19)	0.3979(13)	0.0691(13)	7.60(67)
C(8A)	0.3472(19)	0.6149(14)	0.0007(14)	8.73(72)
C(1B)	0.8874(26)	0.5969(19)	0.3900(18)	3.86(90)
C(1BB)	0.9755(54)	0.5325(38)	0.3837(37)	3.9(19)
C(2B)	1.0632(26)	0.5833(19)	0.4367(19)	5.20(90)
C(2BB)	1.1220(52)	0.6222(37)	0.3716(37)	10.1(18)
C(3B)	1.0161(26)	0.6921(19)	0.3725(19)	9.25(90)
C(3BB)	0.9699(50)	0.6444(37)	0.4459(37)	7.1(18)
C(4B)	1.0329(26)	0.5791(18)	0.3071(19)	6.84(89)
C(4BB)	0.9478(52)	0.6487(38)	0.3167(39)	5.7(19)
C(5B)	0.8704(17)	0.5211(12)	0.3906(12)	6.60(57)
C(6B)	1.1790(18)	0.6017(13)	0.4278(13)	7.57(69)
C(7B)	0.9992(22)	0.7231(15)	0.4443(16)	10.43(87)
C(8B)	0.9622(19)	0.5999(13)	0.2435(14)	8.63(73)
C(1C)	0.4359(29)	0.4384(20)	0.3251(21)	5.9(10)
C(1CC)	0.3685(43)	0.3697(32)	0.3238(30)	8.5(15)
C(2C)	0.3828(29)	0.3720(21)	0.4351(20)	7.6(10)
C(2CC)	0.4543(45)	0.4352(31)	0.4353(31)	7.0(15)
C(3C)	0.4496(29)	0.3108(21)	0.3366(21)	7.1(10)
C(3CC)	0.4700(43)	0.3163(31)	0.4258(31)	8.9(15)
C(4C)	0.5589(29)	0.3901(21)	0.4121(21)	8.1(10)
C(4CC)	0.5536(45)	0.3873(30)	0.3247(31)	6.8(15)
C(5C)	0.3427(20)	0.4372(14)	0.2868(14)	8.74(72)
C(6C)	0.3712(18)	0.4444(13)	0.4736(13)	6.85(63)
C(7C)	0.4752(18)	0.2505(17)	0.3832(13)	9.12(65)
C(8C)	0.6487(20)	0.3960(14)	0.3578(14)	8.96(73)

one set of α-carbons had unexpectedly low B-values, while the other set had unexpectedly high values. We now realized that the disorder was not of the 50%/50% variety. Rather, one orientation was favored over the other. We now reset the B-values of all α-carbon atoms to 7.0 Å^2 (midway between that of the central nitrogen atom and the average value of the peripheral β-carbons) and refined the occupancies of the α-carbon atoms. These were later fixed, while the individual B-values were refined.

The function $\Sigma w(|F_o| - |F_c|)^2$ was minimized during the full-matrix least-squares refinement. Here $1/w = [\sigma(|F_o|)]^2 + [0.015|F_o|]^2$. Residuals used below are defined as in eqs. 1–3; here, NO is the number of observations and NV is the number of variables.

$$R_F(\%) = 100\,\Sigma||F_o| - |F_c||/\Sigma|F_o| \tag{1}$$

$$R_{wF}(\%) = 100\left[\Sigma w(|F_o| - |F_c|)^2/\Sigma w|F_o|^2\right]^{1/2} \tag{2}$$

$$GOF = \left[\Sigma w(|F_o| - |F_c|)^2/(NO - NV)\right]^{1/2} \tag{3}$$

Refinement of positional parameters, anisotropic thermal parameters for Bi, Fe and O atoms and isotropic thermal parameters for N and C atoms led to conver-

TABLE 3

ANISOTROPIC THERMAL PARAMETERS FOR $[Et_4N^+]_3[BiFe_4(CO)_{16}^{3-}]$ [a]

Atom	B_{11}	B_{22}	B_{33}	B_{12}	B_{13}	B_{23}
Bi	2.392(25)	2.823(27)	3.186(26)	−0.007(42)	0.596(18)	−0.054(42)
Fe(1)	2.67(12)	3.85(13)	3.72(13)	0.57(11)	0.71(10)	−0.38(11)
Fe(2)	3.23(10)	4.42(12)	3.44(10)	0.29(18)	1.000(83)	0.06(17)
Fe(3)	2.94(12)	3.41(13)	3.95(13)	−0.48(11)	0.78(10)	−0.21(11)
Fe(4)	3.46(13)	2.89(13)	4.13(14)	0.01(11)	0.66(11)	0.21(11)
O(11)	6.21(90)	4.52(87)	12.1(14)	−0.12(75)	−2.77(90)	0.76(88)
O(12)	5.94(85)	8.0(10)	9.2(11)	0.06(74)	3.01(79)	3.14(87)
O(13)	5.78(82)	12.6(15)	5.95(84)	1.55(81)	−0.08(68)	−3.84(86)
O(14)	4.98(79)	8.9(11)	7.5(10)	2.40(79)	−0.52(72)	0.37(82)
O(21)	9.6(11)	6.6(10)	5.09(81)	−2.78(86)	1.92(74)	−1.57(71)
O(22)	6.16(86)	9.4(12)	7.9(10)	3.60(85)	3.09(74)	4.53(91)
O(23)	4.43(70)	9.0(12)	7.57(85)	−0.21(70)	0.71(63)	−2.78(78)
O(24)	8.45(94)	10.6(11)	5.90(75)	−0.3(12)	3.80(68)	−1.8(11)
O(31)	8.5(10)	6.20(95)	7.2(10)	−0.57(80)	1.70(78)	2.32(77)
O(32)	4.66(71)	5.6(10)	8.5(10)	0.78(62)	−1.28(68)	0.11(68)
O(33)	3.62(68)	8.6(11)	7.9(10)	0.29(70)	3.33(67)	−1.24(80)
O(34)	6.10(87)	7.1(10)	6.99(94)	−0.24(77)	0.20(73)	−2.11(80)
O(41)	9.2(10)	4.58(81)	6.02(86)	0.87(76)	2.00(78)	0.54(68)
O(42)	6.7(10)	7.8(11)	9.3(11)	−1.30(84)	−3.11(87)	−0.60(89)
O(43)	3.87(72)	7.2(10)	11.6(12)	2.80(71)	1.70(77)	1.78(87)
O(44)	14.2(15)	4.90(91)	8.5(11)	−1.2(10)	0.9(10)	3.07(83)

[a] These are in standard Syntex XTL format and enter the expression for the calculated structure factor in the form: $\exp[-0.25(h^2a^{*2}B_{11} + \ldots 2hka^*b^*B_{12} + \ldots)]$.

gence with the residuals R_F 7.5%, R_{wF} 6.1% and *GOF* 1.71 for the 4306 data with $|F_o| > 3\sigma(|F_o|)$; R_F 5.2%, R_{wF} 5.4% and *GOF* 1.74 for those 3342 data with $|F_o| > 6\sigma(|F_o|)$. It should be noted that the heaviest atom in the structure, Bi with $Z = 83$, lies at $x = -0.0146$, $y = 0.24895$ and $z = 0.22798$. This is sufficiently close to the pseudo-special position, 0, 1/4, 1/4, that all data with $h + l = 2n + 1$ are extremely weak. (Average $|E|$ values, by parity group, are 1.639 for eoe, 1.546 for ooo, 1.540 for oeo, 1.413 for eee, 0.263 for eoo, 0.248 for eeo, 0.246 for ooe and 0.227 for oee).

Throughout the analysis, the analytical form of the scattering factors for neutral Bi, Fe, O, N and C atoms were used [10a]; these were corrected for both the real ($\Delta f'$) and imaginary ($i\Delta f''$) components of anomalous dispersion [10b]. Contributions from hydrogen atoms were not included in the analysis (there are a total of 120 locations, each of partial occupancy, for the 60 hydrogen atoms contained in the 3 independent $[Et_4N^+]$ ions). Final atomic positional and thermal parameters are collected in Tables 2 and 3.

Description of the structure of $[Et_4N^+]_3[BiFe_4(CO)_{16}^{3-}]$

Crystals are composed of isolated $[BiFe_4(CO)_{16}^{3-}]$ anions and $[Et_4N^+]$ cations (in a 1/3 ratio), separated by normal Van der Waals' distances. There are no abnormally short inter-ionic contacts. A labelling diagram for the $[BiFe_4(CO)_{16}^{3-}]$ anion is provided by Fig. 1, while Fig. 2 provides a stereoscopic view of this anion. Interatomic distances and angles are compiled in Tables 4 and 5.

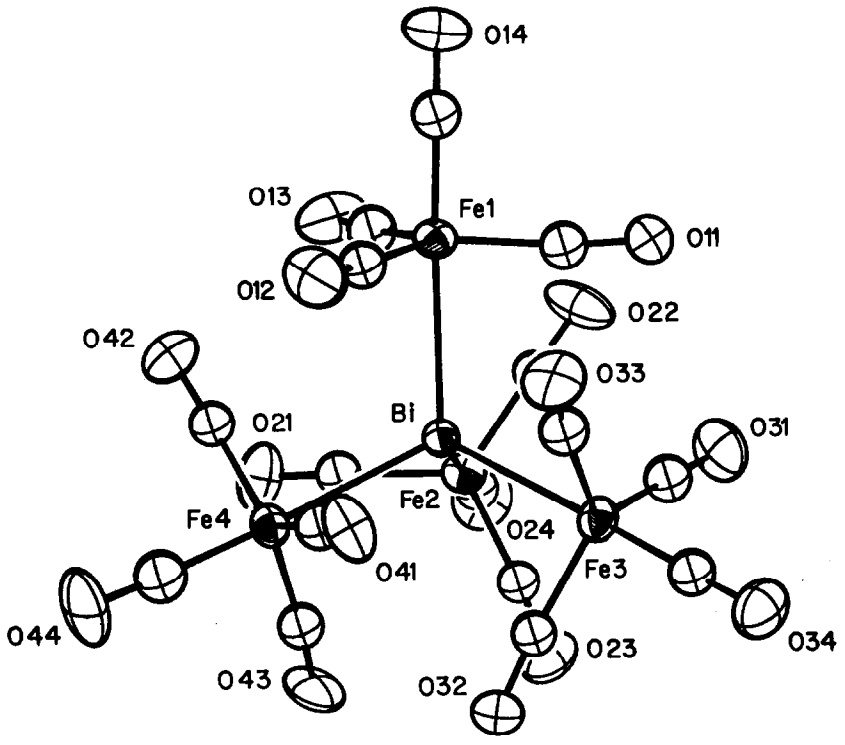

Fig. 1. Labeling diagram for the $[BiFe_4(CO)_{16}^{3-}]$ anion. Carbon atoms of the carbonyl groups are numbered as their attached oxygen atoms; thus C(11) is linked to O(11), etc. [ORTEP-II diagram.].

The $[BiFe_4(CO)_{16}^{3-}]$ anion may be regarded as a central Bi^V atom tetrahedrally surrounded by four $Fe(CO)_4^{2-}$ units. Angles about bismuth range from 108.38(8) through 110.69(8)°, with an average Fe–Bi–Fe angle of 109.47°. The individual

(Continued on p. 108)

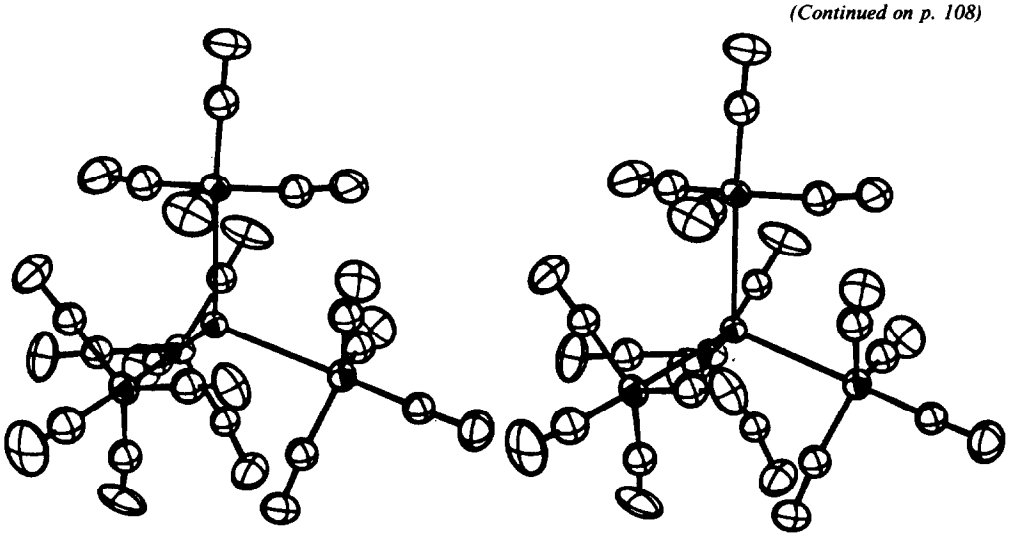

Fig. 2. Stereoscopic view of the $[BiFe_4(CO)_{16}^{3-}]$ ion.

TABLE 4

INTERATOMIC DISTANCES (Å) FOR $[Et_4N^+]_3[BiFe_4(CO)_{16}^{3-}]$

(A) Bismuth – iron distances			
Bi–Fe(1)	2.753(3)	Bi–Fe(3)	2.751(3)
Bi–Fe(2)	2.748(2)	Bi–Fe(4)	2.749(3)
(B) Equatorial Fe – C and C – O distances			
Fe(1)–C(11)	1.755(22)	C(11)–O(11)	1.169(27)
Fe(1)–C(12)	1.812(19)	C(12)–O(12)	1.131(25)
Fe(1)–C(13)	1.800(21)	C(13)–O(13)	1.135(26)
Fe(2)–C(21)	1.787(24)	C(21)–O(21)	1.144(28)
Fe(2)–C(22)	1.755(21)	C(22)–O(22)	1.168(26)
Fe(2)–C(23)	1.767(18)	C(23)–O(23)	1.162(22)
Fe(3)–C(31)	1.773(22)	C(31)–O(31)	1.176(27)
Fe(3)–C(32)	1.768(19)	C(32)–O(32)	1.178(23)
Fe(3)–C(33)	1.859(22)	C(33)–O(33)	1.119(26)
Fe(4)–C(41)	1.729(22)	C(41)–O(41)	1.179(26)
Fe(4)–C(42)	1.745(19)	C(42)–O(42)	1.175(26)
Fe(4)–C(43)	1.788(21)	C(43)–O(43)	1.149(25)
(C) Axial Fe – C and C – O distances			
Fe(1)–C(14)	1.718(21)	C(14)–O(14)	1.168(26)
Fe(2)–C(24)	1.759(18)	C(24)–O(24)	1.161(22)
Fe(3)–C(34)	1.667(20)	C(34)–O(34)	1.218(25)
Fe(4)–C(44)	1.701(23)	C(44)–O(44)	1.166(28)
(D) N – C distances in the Et_4N^+ cations			
N(1)–C(1A)	1.62(4)	N(1)–C(1AA)	1.55(6)
N(1)–C(2A)	1.59(4)	N(1)–C(2AA)	1.56(6)
N(1)–C(3A)	1.53(4)	N(1)–C(3AA)	1.79(6)
N(1)–C(4A)	1.58(4)	N(1)–C(4AA)	1.58(6)
N(2)–C(1B)	1.65(4)	N(2)–C(1BB)	1.65(8)
N(2)–C(2B)	1.49(4)	N(2)–C(2BB)	1.59(7)
N(2)–C(3B)	1.57(4)	N(2)–C(3BB)	1.54(7)
N(2)–C(4B)	1.57(4)	N(2)–C(4BB)	1.56(8)
N(3)–C(1C)	1.51(4)	N(3)–C(1CC)	1.56(6)
N(3)–C(2C)	1.59(4)	N(3)–C(2CC)	1.61(6)
N(3)–C(3C)	1.56(4)	N(3)–C(3CC)	1.62(6)
N(3)–C(4C)	1.53(4)	N(3)–C(4CC)	1.60(6)
(E) C – C distances in the Et_4N^+ cations			
C(1A)–C(5A)	1.62(5)	C(1AA)–C(5A)	1.73(7)
C(2A)–C(6A)	1.70(5)	C(2AA)–C(6A)	1.54(7)
C(3A)–C(7A)	1.52(5)	C(3AA)–C(7A)	1.53(7)
C(4A)–C(8A)	1.54(5)	C(4AA)–C(8A)	1.55(7)
C(1B)–C(5B)	1.51(4)	C(1BB)–C(5B)	1.45(8)
C(2B)–C(6B)	1.62(4)	C(2BB)–C(6B)	1.38(8)
C(3B)–C(7B)	1.53(5)	C(3BB)–C(7B)	1.61(8)
C(4B)–C(8B)	1.59(5)	C(4BB)–C(8B)	1.72(8)
C(1C)–C(5C)	1.45(5)	C(1CC)–C(5C)	1.55(7)
C(2C)–C(6C)	1.62(5)	C(2CC)–C(6C)	1.37(7)
C(3C)–C(7C)	1.53(5)	C(3CC)–C(7C)	1.54(7)
C(4C)–C(8C)	1.62(5)	C(4CC)–C(8C)	1.43(7)

TABLE 5

INTERATOMIC ANGLES (°) FOR $[Et_4N^+]_3[BiFe_4(CO)_{16}^{3-}]$

(A) Iron – bismuth – iron angles

Fe(1)–Bi–Fe(2)	110.69(8)	Fe(2)–Bi–Fe(3)	109.08(8)
Fe(1)–Bi–Fe(3)	108.89(8)	Fe(2)–Bi–Fe(4)	109.51(8)
Fe(1)–Bi–Fe(4)	110.25(8)	Fe(3)–Bi–Fe(4)	108.38(8)

(B) Bismuth – iron – carbon angles

Bi–Fe(1)–C(11)	85.3(7)	Bi–Fe(3)–C(31)	86.0(7)
Bi–Fe(1)–C(12)	86.4(6)	Bi–Fe(3)–C(32)	86.3(6)
Bi–Fe(1)–C(13)	87.9(7)	Bi–Fe(3)–C(33)	84.9(7)
Bi–Fe(1)–C(14)	175.7(7)	Bi–Fe(3)–C(34)	177.2(7)
Bi–Fe(2)–C(21)	86.1(7)	Bi–Fe(4)–C(41)	86.4(7)
Bi–Fe(2)–C(22)	85.3(7)	Bi–Fe(4)–C(42)	85.7(7)
Bi–Fe(2)–C(23)	88.1(6)	Bi–Fe(4)–C(43)	87.7(7)
Bi–Fe(2)–C(24)	176.7(7)	Bi–Fe(4)–C(44)	176.7(8)

(C) Carbon – iron – carbon angles

C(11)–Fe(1)–C(12)	122.9(9)	C(31)–Fe(3)–C(32)	118.5(9)
C(11)–Fe(1)–C(13)	118.4(10)	C(31)–Fe(3)–C(33)	120.6(10)
C(11)–Fe(1)–C(14)	92.5(10)	C(31)–Fe(3)–C(34)	96.9(10)
C(12)–Fe(1)–C(13)	117.6(9)	C(32)–Fe(3)–C(33)	119.2(9)
C(12)–Fe(1)–C(14)	91.7(9)	C(32)–Fe(3)–C(34)	92.2(9)
C(13)–Fe(1)–C(14)	96.4(10)	C(33)–Fe(3)–C(34)	93.8(10)
C(21)–Fe(2)–C(22)	124.4(10)	C(41)–Fe(4)–C(42)	122.5(10)
C(21)–Fe(2)–C(23)	116.7(9)	C(41)–Fe(4)–C(43)	117.2(10)
C(21)–Fe(2)–C(24)	93.3(10)	C(41)–Fe(4)–C(44)	91.5(10)
C(22)–Fe(2)–C(23)	117.8(9)	C(42)–Fe(4)–C(43)	119.2(9)
C(22)–Fe(2)–C(24)	92.4(10)	C(42)–Fe(4)–C(44)	93.3(10)
C(23)–Fe(2)–C(24)	95.1(9)	C(43)–Fe(4)–C(44)	95.5(10)

(D) Iron – carbon – oxygen angles

Fe(1)–C(11)–O(11)	173.1(19)	Fe(3)–C(31)–O(31)	173.3(19)
Fe(1)–C(12)–O(12)	176.9(18)	Fe(3)–C(32)–O(32)	174.9(17)
Fe(1)–C(13)–O(13)	174.7(19)	Fe(3)–C(33)–O(33)	170.9(20)
Fe(1)–C(14)–O(14)	175.6(19)	Fe(3)–C(34)–O(34)	176.5(17)
Fe(2)–C(21)–O(21)	174.4(20)	Fe(4)–C(41)–O(41)	175.6(19)
Fe(2)–C(22)–O(22)	173.0(18)	Fe(4)–C(42)–O(42)	177.8(18)
Fe(2)–C(23)–O(23)	174.4(16)	Fe(4)–C(43)–O(43)	175.4(19)
Fe(2)–C(24)–O(24)	178.1(19)	Fe(4)–C(44)–O(44)	175.5(20)

(E) Carbon – nitrogen – carbon angles in Et_4N^+ cations

C(1A)–N(1)–C(2A)	103.5(22)	C(1AA)–N(1)–C(2AA)	103.5(33)
C(1A)–N(1)–C(3A)	103.3(22)	C(1AA)–N(1)–C(3AA)	103.1(31)
C(1A)–N(1)–C(4A)	115.0(22)	C(1AA)–N(1)–C(4AA)	119.2(34)
C(2A)–N(1)–C(3A)	112.7(23)	C(2AA)–N(1)–C(3AA)	113.6(31)
C(2A)–N(1)–C(4A)	109.8(22)	C(2AA)–N(1)–C(4AA)	112.6(33)
C(3A)–N(1)–C(4A)	112.2(23)	C(3AA)–N(1)–C(4AA)	104.8(31)
C(1B)–N(2)–C(2B)	107.8(21)	C(1BB)–N(2)–C(2BB)	111.0(37)
C(1B)–N(2)–C(3B)	107.1(21)	C(1BB)–N(2)–C(3BB)	104.3(38)
C(1B)–N(2)–C(4B)	106.9(20)	C(1BB)–N(2)–C(4BB)	111.8(38)
C(2B)–N(2)–C(3B)	113.0(22)	C(2BB)–N(2)–C(3BB)	109.8(38)
C(2B)–N(2)–C(4B)	111.4(22)	C(2BB)–N(2)–C(4BB)	111.9(39)

continued

TABLE 5 (continued)

C(3B)–N(2)–C(4B)	110.4(21)	C(3BB)–N(2)–C(4BB)	107.6(39)
C(1C)–N(3)–C(2C)	113.9(23)	C(1CC)–N(3)–C(2CC)	119.9(32)
C(1C)–N(3)–C(3C)	111.5(23)	C(1CC)–N(3)–C(3CC)	109.5(32)
C(1C)–N(3)–C(4C)	112.1(23)	C(1CC)–N(3)–C(4CC)	105.6(32)
C(2C)–N(3)–C(3C)	101.5(22)	C(2CC)–N(3)–C(3CC)	94.4(31)
C(2C)–N(3)–C(4C)	103.4(23)	C(2CC)–N(3)–C(4CC)	115.1(32)
C(3C)–N(3)–C(4C)	113.7(23)	C(3CC)–N(3)–C(4CC)	111.9(32)
(F) Nitrogen – carbon – carbon angles in Et_4N^+ cations			
N(1)–C(1A)–C(5A)	103.1(25)	N(1)–C(1AA)–C(5A)	101.3(36)
N(1)–C(2A)–C(6A)	102.8(25)	N(1)–C(2AA)–C(6A)	112.4(39)
N(1)–C(3A)–C(7A)	115.8(28)	N(1)–C(3AA)–C(7A)	102.4(34)
N(1)–C(4A)–C(8A)	109.0(27)	N(1)–C(4AA)–C(8A)	107.9(39)
N(2)–C(1B)–C(5B)	109.9(24)	N(2)–C(1BB)–C(5B)	113.5(47)
N(2)–C(2B)–C(6B)	109.0(24)	N(2)–C(2BB)–C(6B)	116.7(49)
N(2)–C(3B)–C(7B)	109.0(25)	N(2)–C(3BB)–C(7B)	107.0(43)
N(2)–C(4B)–C(8B)	114.1(25)	N(2)–C(4BB)–C(8B)	107.4(43)
N(3)–C(1C)–C(5C)	118.4(29)	N(3)–C(1CC)–C(5C)	109.7(38)
N(3)–C(2C)–C(6C)	108.6(25)	N(3)–C(2CC)–C(6C)	122.5(43)
N(3)–C(3C)–C(7C)	113.6(28)	N(3)–C(3CC)–C(7C)	109.6(38)
N(3)–C(4C)–C(8C)	110.9(27)	N(3)–C(4CC)–C(8C)	117.4(41)

bismuth–iron bond lengths are Bi–Fe(1) 2.753(3), Bi–Fe(2) 2.748(2), Bi–Fe(3) 2.751(3) and Bi–Fe(4) 2.749(3) Å (average Bi–Fe 2.750 ± 0.002 Å). This may be compared with the pendant Bi–$Fe(CO)_4$ bond length of 2.752(6) Å in the $[Bi_4Fe_4(CO)_{13}^{2-}]$ ion [3], the nine core Bi–Fe distances of 2.699(6)–2.753(6) Å in the same $[Bi_4Fe_4(CO)_{13}^{2-}]$ ion [3], the Bi–Fe distances of 2.648(2)–2.652(1) Å in the tetrahedral $[BiFe_3(CO)_9(\mu_3\text{-}CO)^-]$ cluster [1] and Bi–Fe distances of 2.617(2)–2.643(2) Å in the trigonal-bipyramidal metal cluster $Bi_2Fe_3(CO)_9$ [2].

Each iron atom is in an approximately trigonal-bipyramidal environment; in each case the bismuth atom and a carbonyl ligand are in axial sites while a further three carbonyl ligands occupy the equatorial positions. Equatorial Fe–CO distances range from 1.729(22) through 1.859(22) Å (average 1.778 ± 0.035 Å) while the axial Fe–CO distance range from 1.667(20) through 1.759(18) Å (average 1.711 ± 0.038 Å). This result indicates that the bismuth atom does not compete effectively for back-donation or π-electron density from the iron atom. Each $Fe(CO)_4$ moiety is distorted toward the "inverted umbrella" configuration, with obtuse (OC, axial)–Fe–(CO, equatorial) angles of 91.5(10) through 96.9(10)° (average 93.7 ± 1.8°) and acute Bi–Fe–(CO, equatorial) angles of 84.9(7)–88.1(6)° (average 86.3 ± 1.1°); this behavior is common in $M(CO)_4X$ and $M(CO)_5X$ fragments.

The (OC_{eq})–Fe–(CO_{eq}) angles are all close to 120°, with a range of 116.7(9)–124.4(10)°.

The four Bi–Fe–(CO, axial) angles are close to 180°, individual values being Bi–Fe(1)–C(14) 175.7(7), Bi–Fe(2)–C(24) 176.7(7), Bi–Fe(3)–C(34) 177.2(7) and Bi–Fe(4)–C(44) 176.7(8)°. All Fe–C–O systems are close to linear. Axial Fe–C–O angles are 175.5(20)–178.1(19)°, while equatorial Fe–C–O angles lie in the range 170.9(20)–177.8(18)°.

Taken overall, the $[BiFe_4(CO)_{16}^{3-}]$ anion has close to T_d symmetry – in agree-

ment with its very simple pattern of C–O stretching frequencies (three bands only, at 1962s, 1906m, 1867m [1] in CH_3CN).

The three Et_4N^+ cations are each disordered, as shown in Scheme 1. The labeling scheme is such that (in the case of the ion centered on N(1)) one orientation has N(1) linked to C(1A), C(2A), C(3A) and C(4A), while the other component has N(1) linked to C(1AA), C(2AA), C(3AA) and C(4AA); C(1A) and C(1AA) are bound to the common peripheral β-carbon C(5A). As can be seen in Tables 4 and 5, bond lengths and angles within these disordered cations are all sensible, although of limited precision.

Additional material available

A table of observed and calculated structure factor amplitudes is available upon request from M.R.C.

Acknowledgments

We would like to acknowledge the generous financial support of the National Science Foundation (CHE8421217), the Petroleum Research Fund, administered by the American Chemical Society, and the Robert A. Welch Foundation.

References

1 K.H. Whitmire, C.B. Lagrone, M.R. Churchill, J.C. Fettinger and L.V. Biondi, Inorg. Chem., 23 (1984) 4227.
2 M.R. Churchill, J.C. Fettinger and K.H. Whitmire, J. Organomet. Chem., 284 (1985) 13.
3 K.W. Whitmire, M.R. Churchill and J.C. Fettinger, J. Amer. Chem. Soc., 107 (1985) 1056.
4 G. Etzrodt, R. Boese and G. Schmid, Chem. Ber., 112 (1979) 2574.
5 G. Huttner, U. Weber, L. Zsolnai, Z. Naturforsch. B, 37 (1982) 707.
6 W. Kruppa, D. Blaser, R. Boese and G. Schmid, Z. Naturforsch. B, 37 (1982) 209.
7 A.A. Bhattacharya and S.G. Shore, Organometallics, 2 (1983) 1251.
8 M.R. Churchill, R.A. Lashewycz and F.J. Rotella, Inorg. Chem., 16 (1977) 265.
9 Syntex XTL Operations Manual, 2nd Edition, Syntex Analytical Instruments, Cupertino, California, (U.S.A.) 1976.
10 (a) G. Germain and M.M. Woolfson, Acta Cryst., B24 (1968) 91; (b) G. Germain, P. Main and M.M. Woolfson, Acta Cryst., A27 (1971) 368.
11 International Tables for X-Ray Crystallography, Vol. 4, Kynoch Press, Birmingham, England (1974), (a) pp. 99–101, (b) pp. 149–150.